

1 **Skp1 is a conserved structural component of the meiotic** 2 **synaptonemal complex**

3

4 Lisa E. Kursel*, Kaan Goktepe, Ofer Rog*

5 ORCID: 0000-0001-6558-6194 (OR), 0000-0002-1178-8230 (LEK)

6 School of Biological Sciences and Center for Cell and Genome Sciences, University of Utah,
7 United States.

8

9 * Correspondence: ofer.rog@utah.edu or lisa.kursel@utah.edu

10 330 Aline Wilmot Skaggs Biology Building

11 257 South 1400 East, 201 SB

12 Salt Lake City, UT 84112

13 **Running head:**

14 **Keywords:** meiosis; synaptonemal complex; SCF; evolution; nematodes; Skp1; *P. pacificus*

15

16 **Summary**

17 During sexual reproduction, the parental chromosomes align along their length and exchange
18 genetic information. These processes depend on a chromosomal interface called the
19 synaptonemal complex. The structure of the synaptonemal complex is conserved across
20 eukaryotes, but, surprisingly, the components that make it up are dramatically different in
21 different organisms. Here we find that a protein well known for its role in regulating protein
22 degradation has been moonlighting as a structural component of the synaptonemal complex in
23 the nematode *Pristionchus pacificus*, and that it has likely carried out both of these functions for
24 more than 100 million years.

25

26 **Abstract**

27 The synaptonemal complex (SC) is a meiotic interface that assembles between parental
28 chromosomes and is essential for the formation of gametes. While the dimensions and
29 ultrastructure of the SC are conserved across eukaryotes, its protein components are highly
30 divergent. Recently, an unexpected component of the SC has been described in the nematode
31 *C. elegans*: the Skp1-related proteins SKR-1/2, which are components of the Skp1, Cullin,
32 F-box (SCF) ubiquitin ligase. Here, we find that the role of SKR-1 in the SC is conserved in
33 nematodes. The *P. pacificus* Skp1 ortholog, Ppa-SKR-1, colocalizes with other SC proteins
34 throughout meiotic prophase, where it occupies the middle of the SC. Like in *C. elegans*, the
35 dimerization interface of Ppa-SKR-1 is required for its SC function. A dimerization mutant, *Ppa-*
36 *skr-1^{F105E}*, fails to assemble SC and is almost completely sterile. Interestingly, the evolutionary
37 trajectory of SKR-1 contrasts with other SC proteins. Unlike most SC proteins, SKR-1 is highly
38 conserved in nematodes. Our results suggest that the structural role of SKR-1 in the SC has
39 been conserved since the common ancestor of *C. elegans* and *P. pacificus*, and that rapidly
40 evolving SC proteins have maintained the ability to interact with SKR-1 for at least 100 million
41 years.

42 **Introduction**

43 The synaptonemal complex (SC) is a conserved interface that facilitates chromosome
44 organization during meiosis. The SC aligns parental chromosomes end-to-end and regulates
45 genetic exchanges between them, ultimately allowing for the proper segregation of
46 chromosomes during the meiotic divisions. First identified by electron microscopy over 60 years
47 ago, the SC is made up of two parallel axes (also called lateral or axial elements) separated by
48 repeating striations that make up the central region of the SC (throughout, we refer to the
49 central region of the SC simply as 'the SC' (Page and Hawley 2004; Zickler and Kleckner
50 2015)).

51 Despite its essential role in reproduction and its conserved ultrastructure across sexually
52 reproducing organisms, SC components have diverged beyond recognition in multiple
53 eukaryotic clades (Kursel, Cope, and Rog 2021; Hemmer and Blumenstiel 2016). Indeed, new
54 SC components are still being identified, and we likely still lack the full complement of SC
55 components in most model organisms. Further complicating molecular studies, SC components
56 exhibit near-complete co-dependence for assembly onto chromosomes, in worms and in other
57 organisms (Colaiácovo et al. 2003; MacQueen et al. 2002; Smolikov et al. 2007; Smolikov,
58 Schild-Prüfert, and Colaiácovo 2009; Collins et al. 2014; Page et al. 2008; Schramm et al.

59 2011). Recently, co-expression of SC components allowed their purification from bacteria
60 (Blundon et al. 2024). This suggests that SC subunits intimately associate with one another to
61 form the repeating building blocks of an assembled SC. However, only a few intra-SC
62 interaction interfaces have been defined (Dunce et al. 2018; Dunne and Davies 2019; Sánchez-
63 Sáez et al. 2020; Dunce, Salmon, and Davies 2021; Kursel, Martinez, and Rog 2023), and, due
64 to sequence divergence, it is unclear whether any of them constitute a conserved feature of the
65 SC.

66 Recently, two unexpected SC proteins were identified in *C. elegans*: the Skp1-related
67 proteins SKR-1 and SKR-2 (due to their functional redundancy we refer to them throughout as
68 SKR-1/2; (Blundon et al. 2024)). SKR-1/2 are essential members of the Skp1, Cullin, F-box
69 (SCF) ubiquitin ligase complex, which plays a part in virtually all eukaryotic cellular processes
70 including germline designation (DeRenzo, Reese, and Seydoux 2003), sex determination
71 (Clifford et al. 2000), transcriptional regulation (Ouni, Flick, and Kaiser 2010), circadian
72 oscillation (Han et al. 2004) and hormone signaling in plants (Gray et al. 1999), to name a few
73 (Willems, Schwab, and Tyers 2004). Within the SCF complex, Skp1 acts as an adapter by
74 binding the N-terminus of Cul1 and the F-box motif in the F-box protein, linking the core scaffold
75 to the substrate of the ubiquitin ligase machinery. SKR-1/2 co-purify with all other *C. elegans* SC
76 proteins, localize to the SC, and are required for SC assembly *in vivo*. Notably, the SCF Cullin
77 subunit CUL-1 does not localize to the SC and is not required for SC assembly. These data
78 support the conclusion that SKR-1/2 are *bona fide* SC proteins in *C. elegans* (Blundon et al.
79 2024).

80 Here we address two outstanding questions regarding the role of SKR-1 in the SC. 1) Is
81 the structural role of SKR-1 in the SC conserved in other nematodes? And 2) Does SKR-1 share
82 a similar evolutionary signature to other SC proteins? We identify a single SKR-1 ortholog in the
83 distantly related nematode *Pristionchus pacificus*, Ppa-SKR-1, and find that it localizes to the
84 middle of the SC. Like in *C. elegans*, the predicted dimerization interface in Ppa-SKR-1 is
85 necessary for SC assembly. Our results indicate that Ppa-SKR-1 is a structural component of
86 the SC in *P. pacificus*, suggesting that its role in the SC originated at least 100 million years ago,
87 in the common ancestor of *Pristionchus* and *Caenorhabditis* nematodes. Interestingly, we find
88 that the primary sequence of SKR-1 is conserved, setting it apart from other SC proteins and
89 shedding light on the evolutionary pressures that shape the SC.

90 **Results**

91 *Identifying P. pacificus SKR-1*

92 *C. elegans* and *P. pacificus* are a useful species pair for comparative studies. Like *C.*
93 *elegans*, *P. pacificus* is a free-living, hermaphroditic nematode that has six pairs of
94 chromosomes. Previous studies of meiosis in *P. pacificus* identified two SC proteins; Ppa-SYP-1
95 (Kursel, Cope, and Rog 2021) and Ppa-SYP-4 (Rillo-Bohn et al. 2021). Consistent with the rapid
96 divergence of SC proteins, Ppa-SYP-4 and Ppa-SYP-1 exhibit little to no sequence homology,
97 respectively, with their *C. elegans* counterparts. Given the recent identification of SKR-1/2 as a
98 structural component of the SC in *C. elegans* (Blundon et al. 2024), we wondered whether
99 SKR-1 plays a similar SC role in *P. pacificus*.

100 We used *C. elegans* SKR-1 as a BLASTp query against *P. pacificus* El Paco V3
101 predicted proteins. We identified a single strong hit which we refer to as Ppa-SKR-1. Ppa-SKR-1
102 clusters with *C. elegans* SKR-1/2 on a strongly supported branch to the exclusion of all other
103 Skp1-related proteins in *P. pacificus* (Figure S1). While the *C. elegans* genome contains a
104 recent duplication of SKR-1 called SKR-2 (Blundon et al. 2024), our phylogenetic analysis
105 reveals that *P. pacificus* contains only one copy of SKR-1. We similarly queried seven additional
106 *Pristionchus* proteomes and found that most species have a single SKR-1 ortholog (Figure S2)).
107 We note that *P. pacificus*, like *C. elegans*, encodes many predicted Skp1-related proteins: 32 in
108 *P. pacificus* and 21 in *C. elegans* (Figure S1; (Nayak et al. 2002)). While the expansion of the
109 Skp1 family in nematodes complicates comprehensive tracing of their evolutionary history,
110 SKR-1 orthologs appear to be the most conserved among Skp1-related proteins, and cluster
111 together in a well-supported clade (Figure S2).

112 *Ppa-SKR-1* localizes to the center of the SC

113 We used CRISPR/Cas9 to insert an OLLAS tag on the N-terminus of Ppa-SKR-1 and
114 examined its localization during meiosis (Figure 1). OLLAS::Ppa-SKR-1 appears as threads on
115 meiotic chromosomes from the time of SC assembly at meiotic entry, throughout pachytene (the
116 stage when the SC is completely assembled on all chromosomes), and to diplotene (the
117 extended stage of SC disassembly; Figure 1A). This pattern matches that of other SC proteins
118 (Rillo-Bohn et al. 2021; Kursel, Cope, and Rog 2021). The axis component HOP-1 (Rillo-Bohn
119 et al. 2021) localizes to meiotic chromosomes slightly before OLLAS::Ppa-SKR-1 as faint lines
120 indicative of unpaired chromosomes (Figure 1B). As OLLAS::Ppa-SKR-1 signal begins to
121 overlap with HOP-1, the lines of HOP-1 are brighter, reflecting paired, synapsed chromosomes.
122 During diplotene, OLLAS::Ppa-SKR-1 remains on the bright-staining regions of HOP-1 until the
123 SC fully disassembles.

124 SC proteins occupy stereotypical positions in the ~150nm space separating the two
125 parental chromosomes. Ppa-SYP-1, like its *C. elegans* counterpart, spans the 100nm width of
126 the SC in a head-to-head manner (N-terminus in, C-terminus out) such that staining with a C-
127 terminal epitope produces two parallel lines and N-terminal staining produces a single thread in
128 the middle of the SC (Köhler et al. 2020; Kursel, Cope, and Rog 2021; Schild-Prüfert et al.
129 2011). Using STED super-resolution microscopy, we found that the axis protein HOP-1 formed
130 parallel tracks that are 153nm wide on average (Figure 1C, D) and that Ppa-SKR-1 localized to
131 the central region of the SC, midway between the parallel HOP-1 tracks. These cytological data
132 indicate that, like in *C. elegans*, Ppa-SKR-1 occupies the middle of the SC ladder, where the N-
133 terminus of SYP-1 is located (Figure 1E, (Blundon et al. 2024)).

134 *The Ppa-SKR-1 dimerization interface is required for SC assembly*

135 The essential functions of Skp1 make it challenging to study its role in the SC. *C.*
136 *elegans* worms lacking both SKR-1 and -2 fail to hatch, reflecting the essential roles of SCF in
137 embryogenesis and cell proliferation (Nayak et al. 2002; Blundon et al. 2024). Given that *P.*
138 *pacificus* harbors a single Skp1 ortholog, we predicted that gene deletion would result in
139 embryonic lethality. We therefore wished to generate a separation-of-function allele of
140 *Ppa-skr-1*.

141 Previous studies found that Skp1 dimerizes *via* a conserved hydrophobic interface that is
142 not essential for F-box binding (Kim et al. 2020; Henzl, Thalmann, and Thalmann 1998). In *C.*
143 *elegans*, mutations that disrupt SKR-1/2's ability to dimerize (*skr-1^{F115E}*) cause a complete failure
144 of SC assembly and prevent SKR-1/2 localization to an already formed SC. Importantly, these
145 mutations do not abolish SCF activity, suggesting that SKR-1/2 dimerization is necessary
146 specifically for SC function (Blundon et al. 2024).

147 We used structural homology to predict the dimerization interface in Ppa-SKR-1 (Figure
148 2A). We found that a residue critical for dimerization in *Dictyostelium* Skp1, F97 (Kim et al.
149 2020), aligns closely with F105 in Ppa-SKR-1 (Figure 2A). To test the function of the putative
150 dimerization interface, we used CRISPR/Cas9 to make *ollas::Ppa-skr-1^{F105E}*. Gratifyingly, we
151 easily obtained *ollas::Ppa-skr-1^{F105E}* homozygous animals. Out of 46 F2s singled from
152 heterozygous *ollas::Ppa-skr-1^{F105E}* F1 parents, 12 were homozygous wildtype, 22 were
153 heterozygous and 12 were homozygous for *ollas::Ppa-skr-1^{F105E}*, matching expected Mendelian
154 ratios. This suggests that the F105E mutation does not disrupt SCF functions during
155 development.

156 To evaluate successful completion of meiosis, we counted total progeny in wild-type,
157 *ollas::Ppa-skr-1* and *ollas::Ppa-skr-1^{F105E}* worms. Total progeny produced by *ollas::Ppa-skr-1*
158 worms were comparable to that of the wild-type *P. pacificus*, indicating that the OLLAS insertion
159 did not interfere with meiosis. In contrast, *ollas::Ppa-skr-1^{F105E}* worms were almost sterile,
160 mimicking other SC null mutants (Figure 2B). Notably, several homozygous hermaphrodites
161 produced one to two progeny, further indicating that OLLAS::Ppa-SKR-1^{F105E} can carry out the
162 non-meiotic functions of Skp1 proteins. Together, this analysis indicated that Ppa-SKR-1
163 dimerization is necessary for reproduction.

164 To examine meiotic dysfunction in more detail, we monitored successful formation of
165 crossovers in meiotic prophase. Chromosomes that form a crossover are joined at metaphase
166 of Meiosis I, forming so-called "bivalents" that can be visualized by staining DNA with DAPI.
167 Since *P. pacificus* has six chromosome pairs, successful generation of a crossover on each pair
168 yields six DAPI-staining bodies. We found no significant difference in DAPI body counts
169 between wild-type and *ollas::Ppa-skr-1* worms. They averaged 5.6 and 5.7 DAPI bodies,
170 respectively (Figure 2C). However, *ollas::Ppa-skr-1^{F105E}* worms had a significantly elevated DAPI
171 body count (mean = 10.5) suggesting that failure of chromosome pairing or crossover formation
172 underlies the reduced progeny count in *ollas::Ppa-skr-1^{F105E}* worms (Figure 2D).

173 Cytological examination established that *Ppa-skr-1^{F105E}* worms lack an SC. Meiotic nuclei
174 in the mutant spent an extended duration in the transition zone - the region of the gonad where
175 the SC assembles, marked by crescent-shaped nuclei (Figure 3, compare to Figure 1A, B). An
176 increase in transition zone length is seen in other SC mutants (MacQueen et al. 2002;
177 Colaiácovo et al. 2003; Smolikov et al. 2007; Smolikov, Schild-Prüfert, and Colaiácovo 2009)
178 and is thought to reflect a synapsis checkpoint (Harper et al. 2011). HOP-1 appeared as thin
179 tracks throughout the gonad in *Ppa-skr-1^{F105E}* worms, indicative of chromosomes that were
180 unable to assemble an SC (Figure 3B). Furthermore, Ppa-SYP-1 staining revealed complete
181 lack of SC assembly (Figure 3C). In *C. elegans* and other species, SC components seem to be
182 required for each other's stability (Colaiácovo et al. 2003; Hurlock et al. 2020; Smolikov et al.
183 2007; Smolikov, Schild-Prüfert, and Colaiácovo 2009; Blundon et al. 2024; Z. Zhang et al.
184 2020). Indeed, Ppa-SYP-1 staining was almost completely absent in *ollas::Ppa-skr-1^{F105E}*
185 worms. Moreover, when SC components are present but cannot load onto chromosomes, SC
186 material forms large aggregates called polycomplexes (Page and Hawley 2004). Notably,
187 polycomplexes are absent in *ollas::Ppa-skr-1^{F105E}* worms (Figure 3) and in *C. elegans skr-1^{F115E}*
188 worms (Blundon et al. 2024), suggesting other SC component are not able to assemble in the

189 dimerization mutant. These data indicate that, like in *C. elegans*, SC formation in *P. pacificus*
190 depends on Ppa-SKR-1 dimerization. Taken together with Ppa-SKR-1 localization (Figure 1),
191 our data indicate that Ppa-SKR-1 is a structural component of the *P. pacificus* SC.

192 *Unlike other SC components, SKR-1 sequence is conserved in nematodes*

193 We previously found that SC proteins in nematodes, *Drosophila* and mammals have a
194 unique evolutionary signature; diverged protein sequence but conserved length and position of
195 coiled-coil domains and conserved overall protein length (Kursel, Cope, and Rog 2021). We
196 hypothesized that this evolutionary signature could be explained by the SC mode of assembly,
197 which likely relies on weak multi-valent interactions mediated by coiled-coil domains. Since the
198 sequence requirements for coiled-coil domains are flexible (typically defined as a heptad repeat
199 where the first and fourth residues are hydrophobic and the fifth and seventh are charged or
200 polar), selection to maintain coiled-coil domains could allow for significant sequence divergence.
201 At the time of our analysis, SKR-1 had not been identified as an SC protein. Therefore, we
202 wished to compare the evolutionary signature of SKR-1 to the other SC proteins.

203 Unlike the other SC proteins in *Caenorhabditis* and *Pristionchus*, the sequence of SKR-1
204 is conserved in both clades, ranking in the bottom one percentile for amino acid substitutions
205 per site (Figure 4A). Unsurprisingly, residues involved in CUL-1 binding, F-box protein binding,
206 and the dimerization interface are highly conserved, even between *C. elegans*, *P. pacificus* and
207 *H. sapiens* (Figure 4B). We also found that SKR-1 does not contain conserved coiled-coil
208 domains (Figure 4C, S3A). *Pristionchus* SKR-1 does have a low-scoring predicted coiled-coil
209 domain from amino acids 20 – 47 (Figure S3A). However, AlphaFold does not predict a coiled-
210 coil formed by Ppa-SKR-1 and this coiled-coil signature is not conserved in *Caenorhabditis*
211 (Figure S3A) or in *Dictyostelium*, where the corresponding residues are mostly disordered in the
212 NMR structure (Kim et al. 2020). Together, this argues against the functional importance of
213 coiled-coil domains in SKR-1 (Figure S3B). Lastly, the length of SKR-1 is conserved, like other
214 SC proteins (Figure 4D). Taken together, our analysis indicates that the evolutionary trajectory
215 of SKR-1 is distinct from other SC proteins in *Caenorhabditis* and *Pristionchus* and suggests
216 that its interaction with other SC proteins is mediated by domains other than coiled-coils.

217 **Discussion**

218 We found that SKR-1 is a structural member of the SC in *P. pacificus*. Ppa-SKR-1
219 dynamically localizes to meiotic chromosomes in a manner that is indistinguishable from that of
220 other SC proteins. Like other SC proteins, Ppa-SKR-1 exhibits stereotypic localization relative to

221 the axes: it localizes to the middle of the SC, placing it near the N-terminus of Ppa-SYP-1
222 (Figure 1E). Finally, like in *C. elegans*, the dimerization interface of Ppa-SKR-1 is necessary for
223 SC assembly but not for other essential functions. Taken together, our cytological, functional
224 and phylogenetic data suggest that the function of SKR-1 as a structural component of the SC
225 has been conserved since the common ancestor of *C. elegans* and *P. pacificus*, at least 100
226 million years ago.

227 Our work on the conservation of an SC role for SKR-1 in nematodes raises the
228 possibility that it extends to Skp1 proteins in other clades. Unsurprisingly, proteasome-mediated
229 degradation regulates multiple key steps in meiosis (Ahuja et al. 2017; Rao et al. 2017; Guan et
230 al. 2022) and the proteasome itself localizes to the SC in *C. elegans* and mice (Rao et al. 2017;
231 Ahuja et al. 2017). Skp1 also localizes to the SC in male and female mice (Guan et al. 2020),
232 and in *Arabidopsis* plants where it is called ASK1 (Wang et al. 2004). In both cases, its
233 disruption leads to meiotic defects (Yang et al. 2006). However, the essential functions of the
234 proteasome and Skp1, and the consequent far-ranging effects of their disruption, has made it
235 difficult to parse their role in the protein degradation from any potential structural role in the SC.

236 *C. elegans* has proved to be an especially valuable system for studying the role of Skp1
237 in the SC because it contains two partially redundant paralogs, SKR-1 and SKR-2. Having two
238 SKR-1 paralogs allowed Blundon and Cesar *et al.* to identify the separation-of-function
239 dimerization mutant. We similarly found that a mutation predicted to disrupt Ppa-SKR-1
240 dimerization results in separation of function; worms are viable and have no obvious growth
241 defects indicating SCF functions are intact, but they are sterile due to failure of SC assembly. It
242 will be interesting to explore whether the corresponding Skp1 dimerization interface - which is
243 conserved at the protein sequence level in mammals and plants - would help to generate
244 separation-of-function alleles in other model organisms.

245 The molecular details of SKR-1 interaction with other SC components remain unknown
246 in both *C. elegans* and *P. pacificus*. SKR-1 proteins are not merely recruited to the SC like other
247 so-called 'client' proteins, including the crossover regulator family ZHP-1/2/3/4 (Jantsch et al.
248 2004) and the polo-like kinase PLK-2 (L. Zhang et al. 2018; Harper et al. 2011; Labella et al.
249 2011). For example, the localization pattern of ZHP-1/2/3/4 is distinct from SC proteins and the
250 SC can still assemble in the absence of the ZHPs. In contrast, SKR-1 is essential for SC
251 assembly in both *C. elegans* and *P. pacificus*, and it contributes to the stability of SC
252 components *in vivo* and *in vitro*. Such intimate co-dependence suggests the existence of
253 underlying protein-protein interactions that provide specificity and stability.

254 The protein surfaces that mediate interactions between SC proteins must co-evolve to
255 maintain compatibility. In this light, the high conservation of SKR-1 *versus* the high divergence
256 of other SC components might seem surprising since proteins in complex often have
257 homogenous evolutionary rates (Wong et al. 2008) and genes whose evolutionary rates covary
258 tend to be functionally related (Clark, Alani, and Aquadro 2012). However, a more recent study
259 reported that direct physical interaction is only a weak driver of evolutionary rate covariation
260 (Little, Chikina, and Clark 2024). Moreover, moonlighting proteins that function in multiple
261 complexes can confound such analyses. Taking these factors into account, SKR-1's role in the
262 highly conserved SCF complex might overwhelm any signal of shared evolutionary rates with
263 other SC proteins. In addition, we note that the SC is a condensate (Rog, Köhler, and Dernburg
264 2017), and that many condensates rely on weak, multivalent interactions to recruit and exclude
265 member and non-member components, respectively (Shin and Brangwynne 2017). SC proteins
266 might have multiple, redundant interaction interfaces with SKR-1, each too weak to pose a
267 strong constraint on the primary sequence.

268 The recent duplication of SKR-1 in the lineage leading to *C. elegans* (Blundon et al.
269 2024) could suggest that gene duplication has allowed Skp1 proteins to adopt a novel function -
270 a structural component of the SC. However, our findings suggest that the role of SKR-1 in the
271 SC is more ancient and that a single SKR-1 protein has likely performed both functions in the
272 common ancestor of *C. elegans* and *P. pacificus*. An ancestral dual-function protein suggests
273 that SKR-1 has been subjected to evolutionary pressures to maintain both functions for at least
274 100 million years. Interestingly, SKR-1's dual roles in SCF and the SC entail that mutations in
275 *skr-1* might have pleiotropic effects in development (SCF) *versus* reproduction (SC). If so, *C.*
276 *elegans* may represent a lineage where such intralocus conflict is resolving by gene duplication
277 and specialization (Castellanos, Wickramasinghe, and Betrán 2024). In this scenario, the
278 different structural and functional requirements of the SC *versus* the SCF complex could be
279 divided between SKR-1 and SKR-2, allowing them to eventually differentiate into an SC-
280 dedicated protein and an SCF-dedicated one. Such specialization has likely taken place
281 throughout the broader Skp1-related gene family, which has massively expanded in nematodes
282 (Nayak et al. 2002). Intralocus conflict and related processes provide a leading framework in the
283 evolution of aging (Adler and Bonduriansky 2014), suggesting that the evolutionary trajectory of
284 SKR-1 in nematodes could shed light on the evolution of aging more broadly.

285 **Materials and Methods**

286 *Worm strains and maintenance*

287 We used *Pristionchus pacificus* strain PS312 for the wildtype control and for injections to
288 make *ollas::Ppa-skr-1*. To make *ollas::Ppa-skr-1^{F105E}*, we injected into *ollas::Ppa-skr-1*. All
289 strains were grown at 20°C on NGM agar with OP50 bacteria. We maintained PS312 and
290 *ollas::Ppa-skr-1* in a homozygous state but since *ollas::Ppa-skr-1^{F105E}* was sterile, we maintained
291 it as a heterozygous line by singling animals and genotyping each generation. We consistently
292 observed severe SC defects in one-quarter of the progeny from a heterozygous parent and
293 never observed severe defects in progeny from *ollas::Ppa-skr-1* or PS312 parents. For DAPI
294 body counts, we identified gonads with SC defects in progeny of *ollas::Ppa-skr-1^{F105E}*
295 heterozygous animals, and considered those gonads with severe SC defects to be
296 homozygous. To perform progeny counts of *ollas::Ppa-skr-1^{F105E}*, we singled from a
297 heterozygous parent, counted progeny and genotyped by PCR (see below) after the complete
298 brood was laid.

299 *Identification of P. pacificus SKR-1*

300 We used *C. elegans* SKR-1 as a query in a BLASTp search, implemented on
301 pristionchus.org, of the *P. pacificus* El Paco V3 genome (Dieterich et al. 2007). The top hit was
302 *ppa_stranded_DN29817_c0_g1_i2*, a 166 amino acid protein. We also performed a tBLASTn
303 search using *C. elegans* SKR-1 as a query against the El Paco V4 genome
304 (GCA_000180635.4) implemented on ncbi.nlm.nih.gov. This identified the coding sequence
305 KAF8362560.1, which encodes a 166 amino acid protein identical to
306 *ppa_stranded_DN29817_c0_g1_i2*. When we used the 166 amino acid protein as a query in a
307 BLASTp search of the *C. elegans* proteome, the top hit was *C. elegans* SKR-1 (F46A9.5).

308 We note that performing the same BLASTp search against the *P. pacificus* genome on
309 wormbase.org (Sternberg et al. 2024) produces a top hit to PPA23980, a protein with 1443
310 amino acids that contains a predicted ABC transporter transmembrane domain in its N-terminus
311 and homology to SKR-1 in its C-terminus. We suspect that this is due to an annotation error that
312 merges two genes since wormbase.org also hosts the El Paco V4 genome assembly and the
313 start codon of the 166 amino acid version of SKR-1 is preserved in PPA23980.

314 To confirm that *ppa_stranded_DN29817_c0_g1_i2* is indeed the SKR-1 ortholog in *P.*
315 *pacificus*, we generated a neighbor-joining phylogenetic tree with all hits that resulted from
316 BLASTp search of *P. pacificus* with *C. elegans* SKR-1 (File S1, S2, S3). Since *P. pacificus*
317 *ppa_stranded_DN29817_c0_g1_i2* groups closest with *C. elegans* SKR-1/2 (Figure S1, File
318 S3), it is most likely to be the SKR-1 ortholog. Thus, we refer to
319 *ppa_stranded_DN29817_c0_g1_i2* as Ppa-SKR-1.

320 *Sequence collection, alignment and phylogenetic analysis*

321 We identified *Caenorhabditis* SKR-1 orthologs using the EnSEMBL Compara pipeline
322 implemented on wormbase.org (Harris et al. 2010). We only kept sequences from species with
323 a single predicted ortholog, with the exception of *C. elegans*, which has an SKR-1 paralog,
324 SKR-2, leaving 16 SKR-1 sequences for analysis. We identified *Pristionchus* SKR-1 orthologs
325 by performing BLASTp with *C. elegans* SKR-1 against the eight *Pristionchus* genomes available
326 on Pristionchus.org (Dieterich et al. 2007). We saved the top hit from each search. We used
327 Clustal Omega for all protein alignments and Geneious Tree Builder (neighbor-joining method,
328 Geneious Prime version 2023.2.1) with 100x bootstrap resampling to generate the phylogenies
329 in supplementary Figures 1 and 2. All protein sequences, alignments and trees are available as
330 supplemental data (File S4 – S9).

331 *CRISPR genome editing*

332 We aimed to insert an OLLAS tag in the N-terminus of Ppa-SKR-1, immediately
333 following the start methionine. We made an injection mix containing 1ul Cas9 (IDR, Alt-R S.p.
334 Cas9 Nuclease V3, 10ug/ul), 3.5ul repair template (200uM), 3.5ul annealed tracr/crRNA mix and
335 0.5ul duplex buffer (IDT). We injected the gonads of wildtype (PS312) young adult
336 hermaphrodite *P. pacificus* and singled each injected worm to its own plate. We extracted DNA
337 from ~16 combined F1 worms from each plate and genotyped with primers that span the
338 OLLAS insertion site (LEK1094 GTTTCACAACAACGGCCCTC and LEK1095
339 CTTGATGACGTCACGGGGAA) to identify “jackpot plates” (*i.e.*, plates with high rates of OLLAS
340 insertion). We singled as many F1s as possible from the jackpot plates and genotyped again to
341 identify individual insertion events.

342 To make *ollas::Ppa-skr-1^{F105E}* we followed a similar strategy as above except we injected
343 into *ollas::Ppa-skr-1*. We screened the pooled F1s by doing PCR with primers LEK1111
344 (GAGAAGGGAACAACGTGGGT) and LEK1112 (CGCGCGTCTCATTCAACAAA) and digesting
345 with Mbol. The predicted Cas9 cut site is near an Mbol site in *ollas::skr-1*, so CRISPR repair
346 events could destroy the Mbol site. In this scenario, wildtype plates will have bands that are
347 259, 241 and 92 base pairs in length after Mbol digest but plates that contain CRISPR mutants
348 will also have a 351 base pair band. We singled F1s from plates with the 351 base pair band
349 and did a second round of genotyping with LEK1111 and LEK1112, this time followed by digest
350 with Sall. Animals that contain CRISPR repair events from the injected homology template will
351 gain an Sall site. PCR from wildtype animals will remain undigested (592 base pairs) whereas

352 PCR from a mutant animal will get cut (336 and 256 base pair bands). See Table S1 for a list of
353 primers, crRNAs and repair templates used for CRISPR.

354 *Immunofluorescence and confocal microscopy*

355 We prepared gonads for immunofluorescence and confocal microscopy as we have
356 done previously (Kursel, Cope, and Rog 2021; Phillips, McDonald, and Dernburg 2009). Briefly,
357 we dissected age-matched adult worms in egg buffer with 0.01% Tween-20 and fixed in a final
358 concentration of 1% formaldehyde. We transferred samples to a HistoBond microscope slide,
359 froze for 1 minute on dry ice and quickly immersed the slide in -20°C methanol for one minute.
360 Slides were washed in PBST and blocked in Roche Block (Cat # 11096176001) for 30 minutes
361 at room temperature. We incubated the slides in 80 µl of primary antibody overnight at 4°C.
362 Primary antibody concentrations were as follows: Rabbit anti-PPA-SYP-1 1:500 (Kursel, Cope,
363 and Rog 2021), Rat anti-OLLAS 1:200 (Invitrogen Catalog # MA5-16125), Rabbit anti-PPA-
364 HOP-1 1:300 (Rillo-Bohn et al. 2021). The following day, slides were washed for three rounds of
365 10 minutes in PBST, then incubated in secondary antibody. Secondary antibody concentrations
366 were as follows: Donkey anti-rabbit Cy3 1:500 and Donkey anti-rat Alexa488 1:500 (Jackson
367 ImmunoResearch). Finally, we washed slides in PBST and DAPI and mounted them in NPG-
368 Glycerol. Slides were imaged on a Zeiss LSM880 confocal microscope with Airyscan and a 63 ×
369 1.4 NA oil objective. Confocal images presented in this manuscript are maximum intensity
370 projections.

371 *STED super-resolution microscopy*

372 Gonads for STED microscopy were prepared as for confocal microscopy with the
373 following changes: 1) we omitted DAPI staining, 2) we used Goat anti-Rabbit STAR RED 1:200
374 (Abberior # STRED-1002-500UG) and Goat anti-Rat Alexa 594 1:200 (Jackson
375 ImmunoResearch) as secondaries, and 3) we mounted the samples in Abberior Mount Liquid
376 Antifade (Abberior # MM-2009-2X15ML). Samples were imaged on Abberior STEDYCON
377 mounted on a Nikon Eclipse Ti microscope with a 100 × 1.45 NA oil objective. Line scans were
378 performed in FIJI (Schindelin et al. 2012).

379 *Structural modeling and alignment*

380 We used AlphaFold (Jumper et al. 2021), implemented in ColabFold (Mirdita et al. 2022),
381 to model the structure of full-length Ppa-SKR-1. We used Pymol ((Schrodinger 2015), version
382 2.5.7) to visualize Ppa-SKR-1 and to align it to the *Dictyostelium* Skp1A dimer NMR structure
383 ((Kim et al. 2020), PDB structure 6V88).

384 *Progeny counts*

385 We singled twelve L4s from each genotype and grew them at 20°C. We moved the
386 parents to a fresh plate every day for four days and counted the progeny after allowing them to
387 mature for up to five days. For the *ollas::Ppa-skr-1^{F105E}* genotype, we singled 50 F1s from a
388 heterozygous animal. We moved the F1s to fresh plates daily as described. At the end of the
389 fourth day of egg laying, we identified the homozygous animals among the F1s by genotyping
390 the parent with LEK1111/LEK1112 PCR primers followed by Sall digest as described above. We
391 counted progeny from those animals confirmed to be homozygous mutants.

392 *Calculating divergence, coiled-coil conservation and length conservation*

393 The *Caenorhabditis* and *Pristionchus* proteome values (Figure 4A, 4C and 4D) were
394 published previously (Kursel, Cope, and Rog 2021). We calculated divergence values, coiled-
395 coil conservation scores and coefficient of variation of protein length for SKR-1 as we have done
396 previously for SC proteins (Kursel, Cope, and Rog 2021) using SKR-1 orthologs from
397 *Caenorhabditis* or *Pristionchus* collected as described above.

398 *Statistical analysis*

399 We used an ordinary one-way ANOVA with Tukey's multiple comparisons test to test for
400 differences in total progeny and DAPI body counts between genotypes (Figure 2B and 2C). In
401 Figure 3A, we used an unpaired t test to test for differences in transition zone length.

402 **Data availability**

403 Worm strains generated in this study are available by request. All sequence alignments
404 and phylogenies are included as supplementary data files. Proteome-wide analysis of
405 divergence, coiled-coil scores and protein length variation in *Caenorhabditis* and *Pristionchus*
406 was published previously (Kursel, Cope, and Rog 2021).

407 **Acknowledgements**

408 We would like to thank the Rog Lab for discussions, Abby Dernburg for antibodies and Yumi Kim
409 for discussions and for sharing data prior to publication. Some strains used in this work were
410 provided by the CGC, which is funded by NIH Office of Research Infrastructure Programs (P40
411 OD010440). We acknowledge the HSC Cell Imaging Core at the University of Utah for use of
412 the STED microscope and The University of Utah Center for High Performance Computing for
413 computational resources. KG was supported by the Undergraduate Research Opportunity
414 Program at the University of Utah and by the Biology Research Scholar Award from the School

415 of Biological Sciences. This work was supported by grants R35GM128804 from NIGMS and
416 2219605 from NSF.
417

418 **Figures**

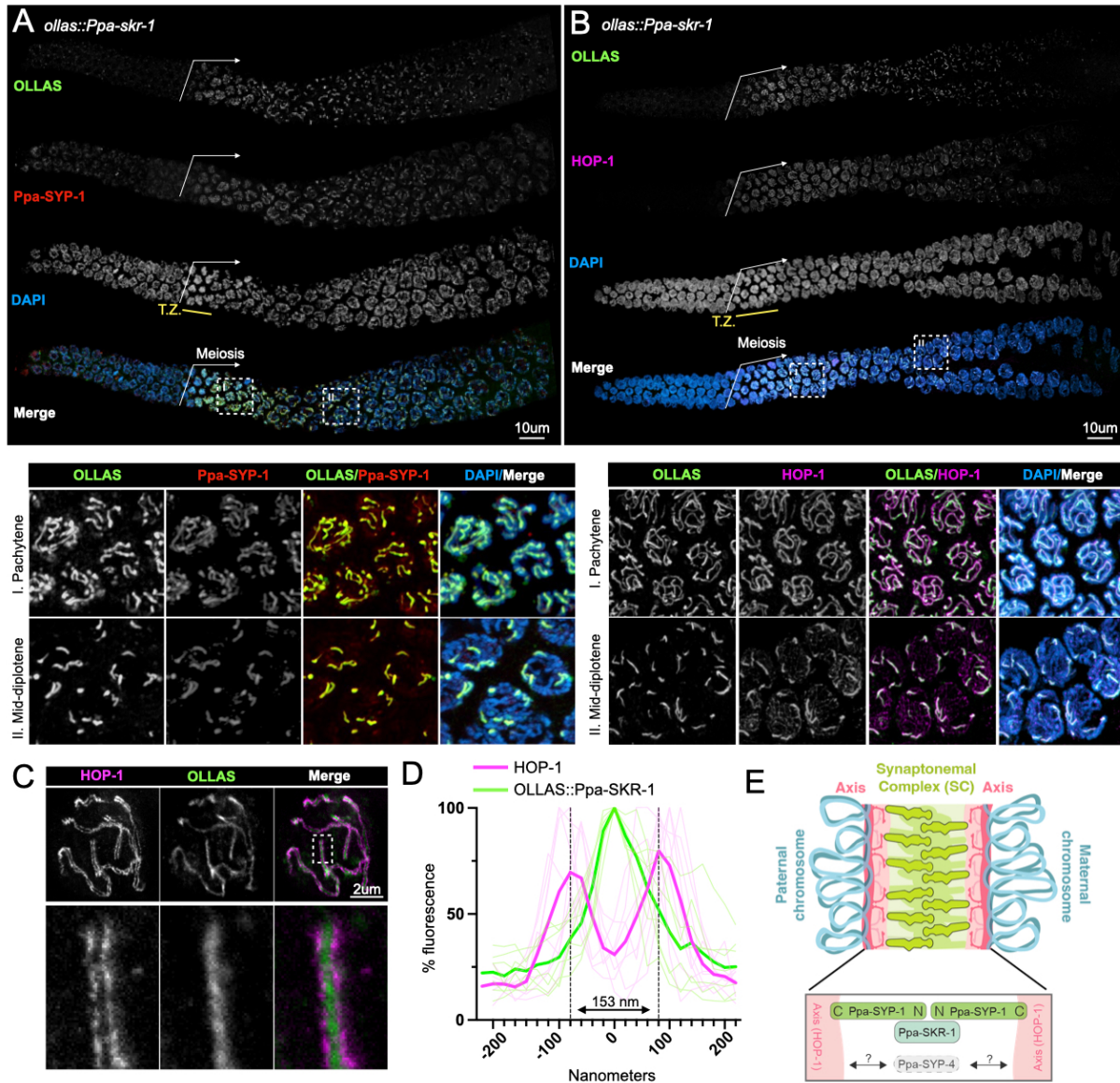


Figure 1: Ppa-SKR-1 localizes to the middle of the SC. (A) Top panel, confocal image of whole gonads from *ollas::Ppa-skr-1* stained with anti-OLLAS, anti-SYP-1 and DAPI. Bottom panel, zoom in on pachytene (I) or mid-diplotene (II) nuclei. (B) Confocal image as in (A) except with HOP-1 staining. In (A) and (B), the beginning of the meiotic gonad is indicated with a white arrow and the transition zone is labeled below the DAPI channel in yellow (T.Z.). (C) Super-resolution STED image of a single pachytene nucleus from *ollas::Ppa-skr-1* worms stained with anti-OLLAS and anti-HOP-1. Zoom-in panels show OLLAS::Ppa-SKR-1 between parallel HOP-1 tracks. (D) Plot of line scans of pixel intensity for anti-HOP-1 and anti-OLLAS across parallel axes in *ollas::Ppa-skr-1* worms. The average distance between parallel axes is 153nm. (E) Cartoon of the *P. pacificus* synaptonemal complex with the orientation and position of Ppa-SYP-1 and Ppa-SKR-1 relative to HOP-1 indicated in the bottom panel. The relative position of Ppa-SYP-4 is not known (grey arrows and question marks). Adapted from (Kursel, Aguayo Martinez, and Rog 2023).

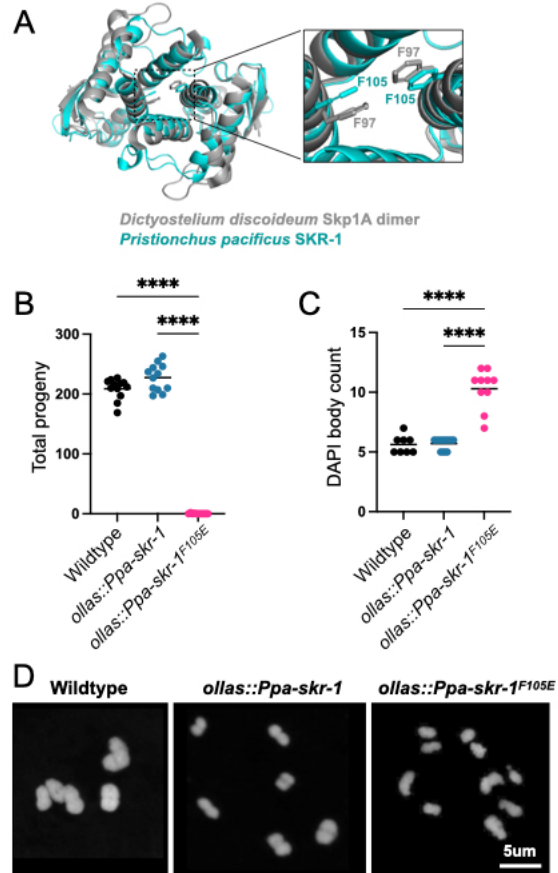


Figure 2: Conserved dimerization interface in SKR-1 is required for *P. pacificus* meiosis. (A) Alignment of *P. pacificus* SKR-1 AlphaFold model (cyan) to *Dictyostelium* Skp1A dimer NMR structure (PDB structure 6V88, gray). Conserved phenylalanines required for dimerization are labeled in zoom. Dot plot depicting total progeny (B) and DAPI body count (C) for wild-type *P. pacificus*, *ollas::Ppa-skr-1* and *ollas::Ppa-skr-1^{F105E}*. Asterisks reflect P-values from Tukey's multiple comparison test where **** indicates $P < 0.0001$. (D) Representative images of DAPI-stained Meiosis I bivalents (DAPI bodies) from the indicated genotypes.

419

420

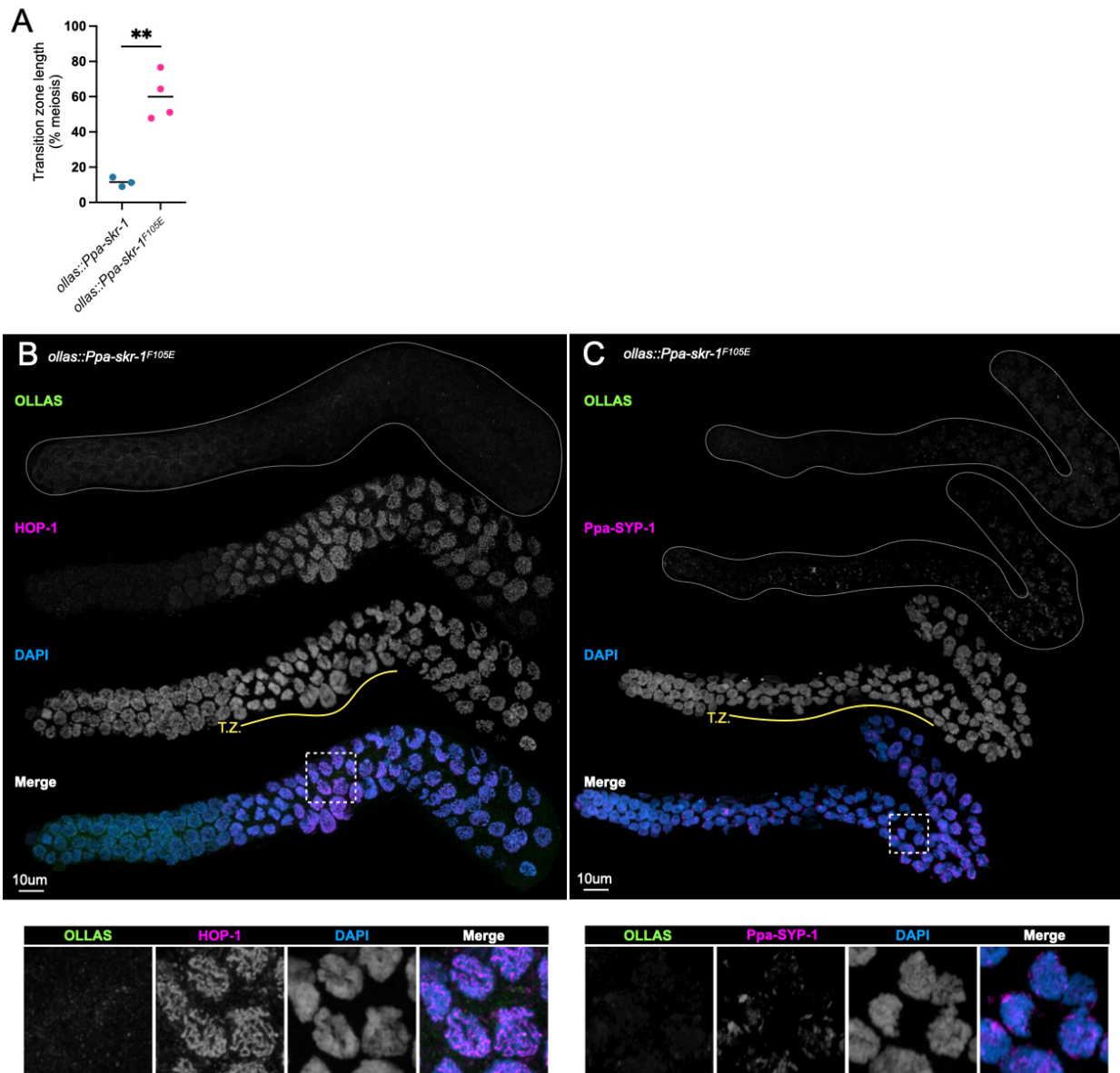


Figure 3: Ppa-SKR-1^{F105E} fails to assemble the SC. (A) Dot plot showing transition zone length as percent of meiosis. Asterisks reflect the P-value from an unpaired T-test where ** indicates $P < 0.01$. (B) and (C), Confocal images of whole gonads from *P. pacificus ollas::skr-1^{F105E}* stained with anti-OLLAS, anti-HOP-1 (B) or anti-SYP-1 (C), and DAPI. Lower panels in (B) and (C) show zoom-in on regions indicated by white, dashed boxes and the transition zone is labeled below the DAPI channel in yellow (T.Z.).

421
422

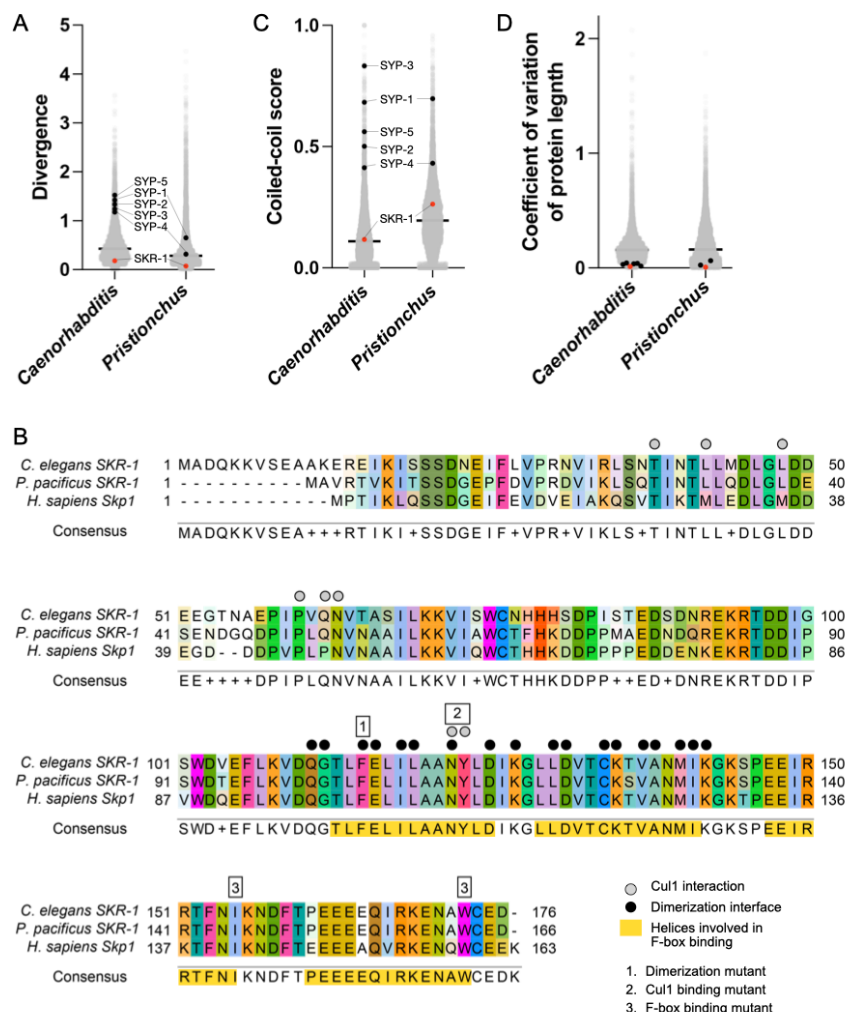


Figure 4: SKR-1 has an evolutionary signature distinct from other SC proteins. (A) Dot plot showing protein divergence for the *Caenorhabditis* and *Pristionchus* proteomes. SYP proteins and SKR-1 are indicated (black and pink, respectively). (B) Alignment of Skp1 orthologs from *C. elegans* and *P. pacificus*, and *H. sapiens* with Cul1 interaction, dimerization and F-box binding sites labeled (Zheng et al. 2002; Kim et al. 2020). Additionally, three mutants generated by Blundon and Caesar *et al.* are indicated by numbered boxes (Blundon et al. 2024). (C) and (D), dot plots showing coiled-coil conservation and coefficient of variation of protein length for the *Caenorhabditis* and *Pristionchus* proteomes. SYP proteins and SKR-1 are indicated as in (A).

423

424

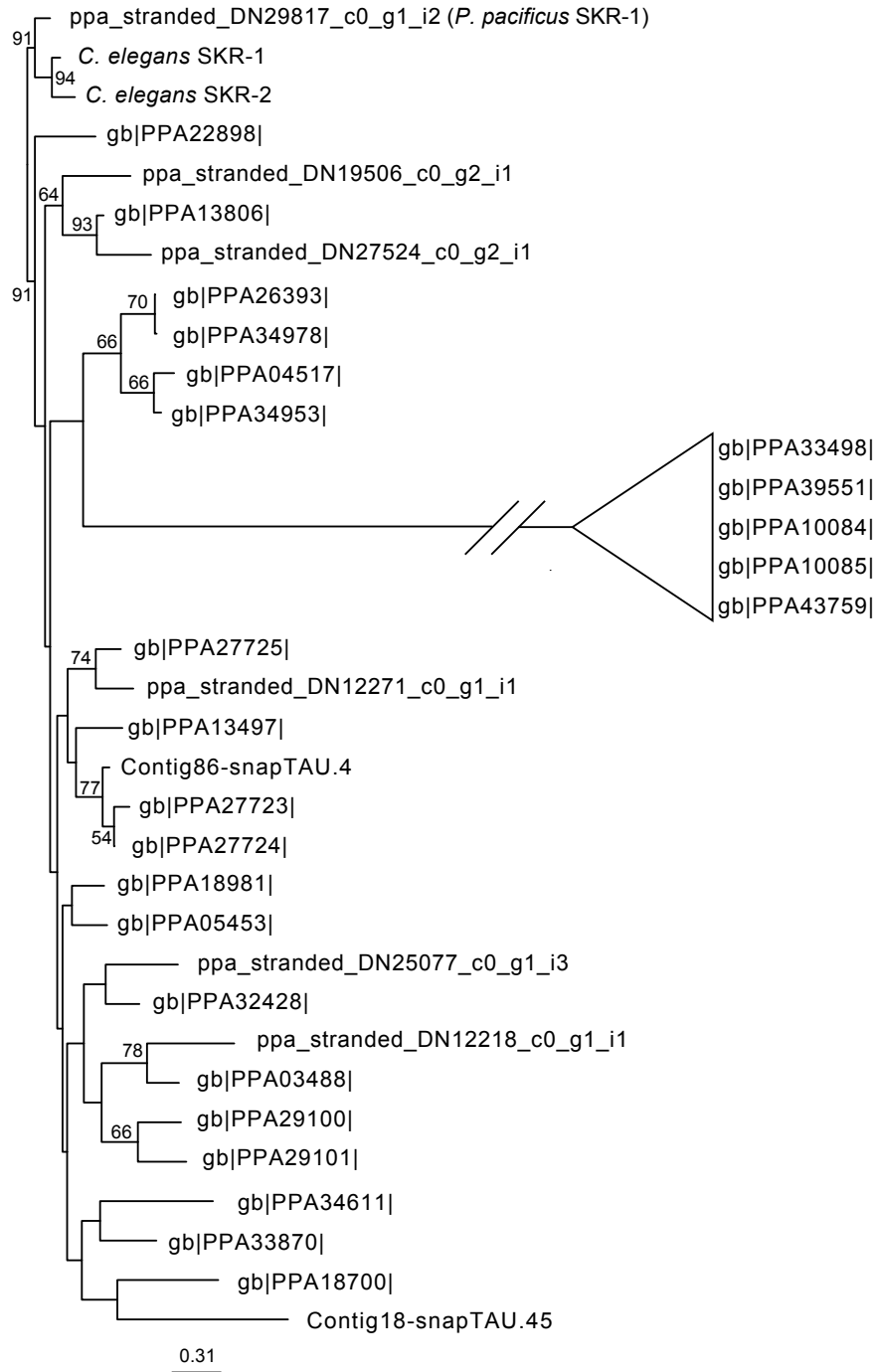


Figure S1: Neighbor-joining phylogenetic tree of *P. pacificus* Skp1-related proteins.

Phylogenetic tree made from a protein alignment of all *P. pacificus* Skp1-related proteins identified via BLASTp search. Bootstrap values greater than 50 are displayed. Note: the branch leading to PPA33498, PPA39551, PPA10084, PPA10085 and PPA43759 was truncated (diagonal lines) to more easily display the entire phylogeny.

425

426

427

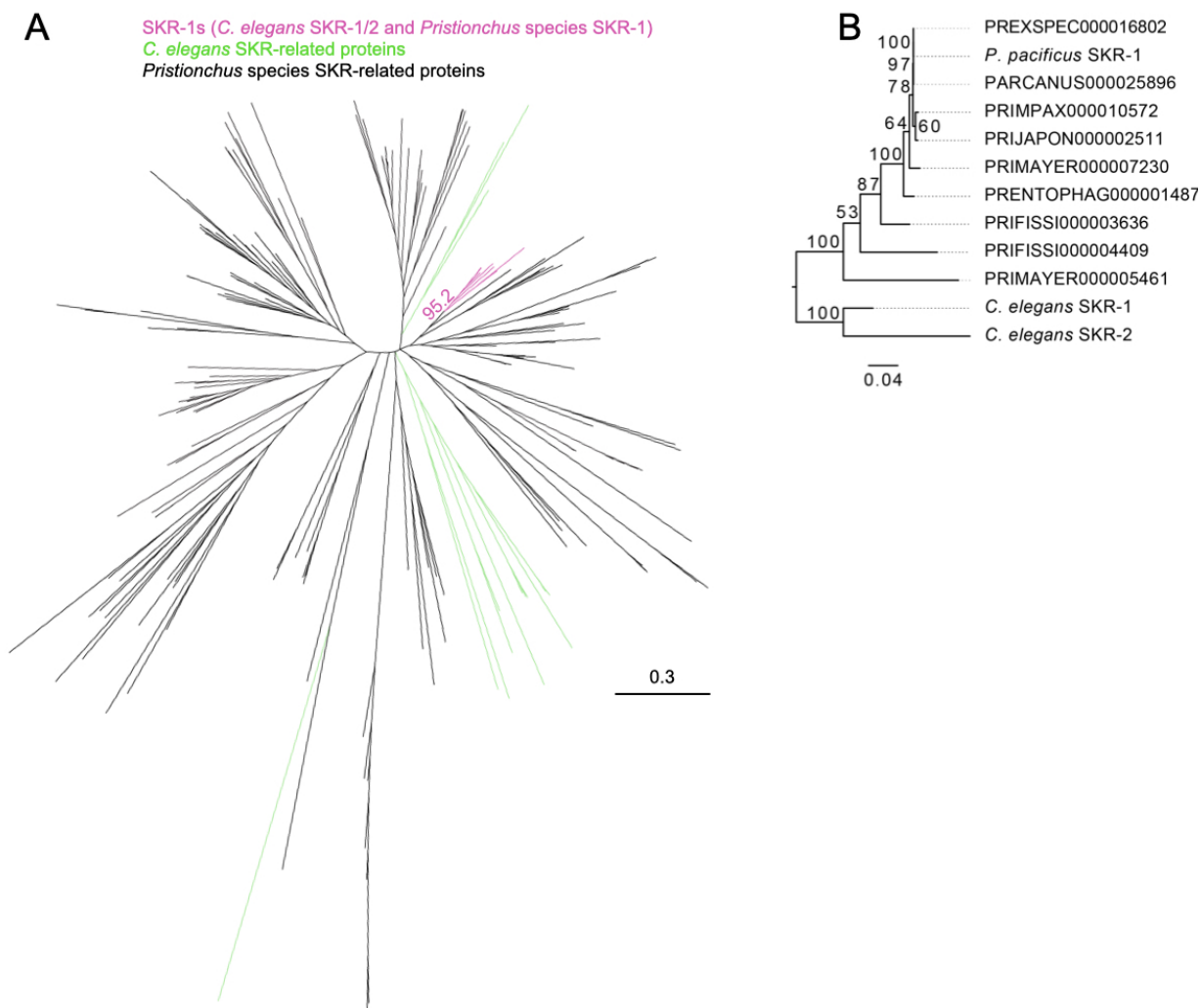


Figure S2: Neighbor-joining phylogenetic tree of *Pristionchus* Skp1-related proteins.

(A) Unrooted phylogenetic tree with 100x bootstrap support made from a protein alignment of all Skp1-related proteins from *C. elegans* and eight *Pristionchus* species. The clade containing *C. elegans* SKR-1/2 and *P. pacificus* SKR-1 has pink branches, all other *C. elegans* SKRs have green branches and all other *Pristionchus* Skp1-related proteins have black branches. The bootstrap support value for the SKR-1 clade is shown. (B) Phylogenetic tree with 100x bootstrap support made from an alignment of the proteins in the SKR-1 clade in (A, pink branches). The tree is rooted on the common ancestor of *Caenorhabditis* and *Pristionchus*.

428

429

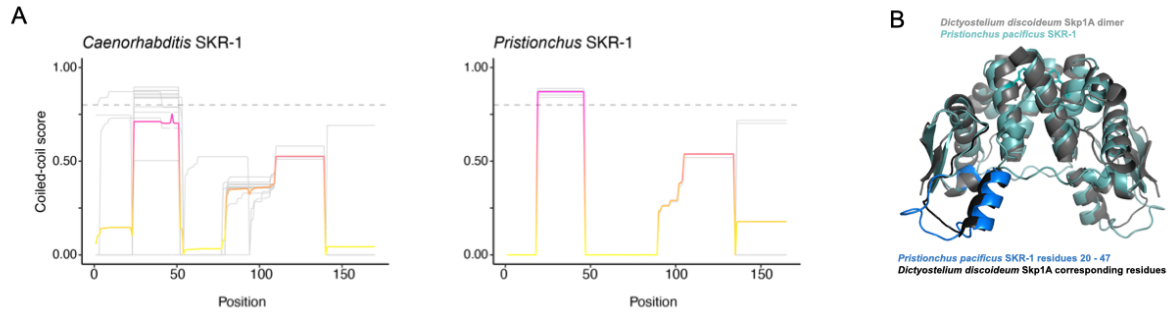


Figure S3: SKR-1 does not contain conserved coiled-coil domains. (A) Plot showing likelihood of coiled-coil domain at every residue in *Caenorhabditis* and *Pristionchus* SKR-1. Individual species are represented by grey lines and the average is shown in a pink to yellow gradient. Higher scores are more likely to be a coiled-coil domain with an arbitrary cut off for a coiled-coil shown in a grey dashed line at 0.8. (B) Structural alignment of *Dictyostelium* Skp1A dimer NMR structure (PDB structure 6V88, gray) and *P. pacificus* SKR-1 (teal) with *P. pacificus* residues 20 – 47 and corresponding residues in *Dictyostelium* labeled in blue and black, respectively.

430

431

432 **Literature cited**

- 433 Adler, Margo I., and Russell Bonduriansky. 2014. "Sexual Conflict, Life Span, and Aging." *Cold*
434 *Spring Harbor Perspectives in Biology* 6 (8).
435 <https://doi.org/10.1101/cshperspect.a017566>.
- 436 Ahuja, Jasvinder S., Rima Sandhu, Rana Mainpal, Crystal Lawson, Hanna Henley, Patricia A.
437 Hunt, Judith L. Yanowitz, and G. Valentin Börner. 2017. "Control of Meiotic Pairing and
438 Recombination by Chromosomally Tethered 26S Proteasome." *Science* 355 (6323):
439 408–11.
- 440 Blundon, Joshua M., Brenda I. Cesar, Jung Woo Bae, Ivana Čavka, Jocelyn Haversat, Jonas
441 Ries, Simone Köhler, and Yumi Kim. 2024. "Skp1 Proteins Are Structural Components of
442 the Synaptonemal Complex in *C. Elegans*." *Science Advances* 10 (7): eadl4876.
- 443 Castellanos, María Del Pilar, Chathuri Devmika Wickramasinghe, and Esther Betrán. 2024. "The
444 Roles of Gene Duplications in the Dynamics of Evolutionary Conflicts." *Proceedings.*
445 *Biological Sciences / The Royal Society* 291 (2024): 20240555.
- 446 Clark, Nathan L., Eric Alani, and Charles F. Aquadro. 2012. "Evolutionary Rate Covariation
447 Reveals Shared Functionality and Coexpression of Genes." *Genome Research* 22 (4):
448 714–20.
- 449 Clifford, R., M. H. Lee, S. Nayak, M. Ohmachi, F. Giorgini, and T. Schedl. 2000. "FOG-2, a Novel
450 F-Box Containing Protein, Associates with the GLD-1 RNA Binding Protein and Directs
451 Male Sex Determination in the *C. Elegans* Hermaphrodite Germline." *Development* 127
452 (24): 5265–76.
- 453 Colaiácovo, Mónica P., Amy J. MacQueen, Enrique Martinez-Perez, Kent McDonald, Adele
454 Adamo, Adriana La Volpe, and Anne M. Villeneuve. 2003. "Synaptonemal Complex
455 Assembly in *C. Elegans* Is Dispensable for Loading Strand-Exchange Proteins but
456 Critical for Proper Completion of Recombination." *Developmental Cell* 5 (3): 463–74.
- 457 Collins, Kimberly A., Jay R. Unruh, Brian D. Slaughter, Zulin Yu, Cathleen M. Lake, Rachel J.
458 Nielsen, Kimberly S. Box, et al. 2014. "Corolla Is a Novel Protein That Contributes to the
459 Architecture of the Synaptonemal Complex of *Drosophila*." *Genetics* 198 (1): 219–28.
- 460 DeRenzo, Cynthia, Kimberly J. Reese, and Geraldine Seydoux. 2003. "Exclusion of Germ
461 Plasm Proteins from Somatic Lineages by Cullin-Dependent Degradation." *Nature* 424
462 (6949): 685–89.

- 463 Dieterich, Christoph, Waltraud Roeseler, Patrick Sobetzko, and Ralf J. Sommer. 2007.
464 "Pristionchus.org: A Genome-Centric Database of the Nematode Satellite Species
465 *Pristionchus Pacificus*." *Nucleic Acids Research* 35 (Database issue): D498-502.
- 466 Dunce, James M., Orla M. Dunne, Matthew Ratcliff, Claudia Millán, Suzanne Madgwick, Isabel
467 Usón, and Owen R. Davies. 2018. "Structural Basis of Meiotic Chromosome Synapsis
468 through SYCP1 Self-Assembly." *Nature Structural & Molecular Biology* 25 (7): 557–69.
- 469 Dunce, James M., Lucy J. Salmon, and Owen R. Davies. 2021. "Structural Basis of Meiotic
470 Chromosome Synaptic Elongation through Hierarchical Fibrous Assembly of SYCE2-
471 TEX12." *Nature Structural & Molecular Biology* 28 (8): 681–93.
- 472 Dunne, Orla M., and Owen R. Davies. 2019. "Molecular Structure of Human Synaptonemal
473 Complex Protein SYCE1." *Chromosoma* 128 (3): 223–36.
- 474 Gray, William M., J. Carlos del Pozo, Loni Walker, Lawrence Hobbie, Eddy Risseeuw, Travis
475 Banks, William L. Crosby, Ming Yang, Hong Ma, and Mark Estelle. 1999. "Identification
476 of an SCF Ubiquitin–Ligase Complex Required for Auxin Response in Arabidopsis
477 *Thaliana*." *Genes & Development* 13 (13): 1678–91.
- 478 Guan, Yongjuan, N. Adrian Leu, Jun Ma, Lukáš Chmátal, Gordon Ruthel, Jordana C. Bloom,
479 Michael A. Lampson, John C. Schimenti, Mengcheng Luo, and P. Jeremy Wang. 2020.
480 "SKP1 Drives the Prophase I to Metaphase I Transition during Male Meiosis." *Science*
481 *Advances* 6 (13): eaaz2129.
- 482 Guan, Yongjuan, Huijuan Lin, N. Adrian Leu, Gordon Ruthel, Serge Y. Fuchs, Luca Busino,
483 Mengcheng Luo, and P. Jeremy Wang. 2022. "SCF Ubiquitin E3 Ligase Regulates DNA
484 Double-Strand Breaks in Early Meiotic Recombination." *Nucleic Acids Research* 50 (9):
485 5129–44.
- 486 Han, Linqi, Mary Mason, Eddy P. Risseeuw, William L. Crosby, and David E. Somers. 2004.
487 "Formation of an SCF(ZTL) Complex Is Required for Proper Regulation of Circadian
488 Timing." *The Plant Journal: For Cell and Molecular Biology* 40 (2): 291–301.
- 489 Harper, Nicola C., Regina Rillo, Sara Jover-Gil, Zoe June Assaf, Needhi Bhalla, and Abby F.
490 Dernburg. 2011. "Pairing Centers Recruit a Polo-like Kinase to Orchestrate Meiotic
491 Chromosome Dynamics in *C. Elegans*." *Developmental Cell* 21 (5): 934–47.

- 492 Harris, Todd W., Igor Antoshechkin, Tamberlyn Bieri, Darin Blasiar, Juancarlos Chan, Wen J.
493 Chen, Norie De La Cruz, et al. 2010. "WormBase: A Comprehensive Resource for
494 Nematode Research." *Nucleic Acids Research* 38 (Database issue): D463-7.
- 495 Hemmer, Lucas W., and Justin P. Blumenstiel. 2016. "Holding It Together: Rapid Evolution and
496 Positive Selection in the Synaptonemal Complex of *Drosophila*." *BMC Evolutionary
497 Biology* 16 (May): 91.
- 498 Henzl, M. T., I. Thalmann, and R. Thalmann. 1998. "OCP2 Exists as a Dimer in the Organ of
499 Corti." *Hearing Research* 126 (1–2): 37–46.
- 500 Hurlock, Matthew E., Ivana Čavka, Lisa E. Kursel, Jocelyn Haversat, Matthew Wooten, Zehra
501 Nizami, Rashi Turniansky, et al. 2020. "Identification of Novel Synaptonemal Complex
502 Components in *C. Elegans*." *The Journal of Cell Biology* 219 (5).
503 <https://doi.org/10.1083/jcb.201910043>.
- 504 Jantsch, Verena, Pawel Pasierbek, Michael M. Mueller, Dieter Schweizer, Michael Jantsch, and
505 Josef Loidl. 2004. "Targeted Gene Knockout Reveals a Role in Meiotic Recombination
506 for ZHP-3, a Zip3-Related Protein in *Caenorhabditis Elegans*." *Molecular and Cellular
507 Biology* 24 (18): 7998–8006.
- 508 Jumper, John, Richard Evans, Alexander Pritzel, Tim Green, Michael Figurnov, Olaf
509 Ronneberger, Kathryn Tunyasuvunakool, et al. 2021. "Highly Accurate Protein Structure
510 Prediction with AlphaFold." *Nature* 596 (7873): 583–89.
- 511 Kim, Hyun W., Alexander Eletsy, Karen J. Gonzalez, Hanke van der Wel, Eva-Maria Strauch,
512 James H. Prestegard, and Christopher M. West. 2020. "Skp1 Dimerization Conceals Its
513 F-Box Protein Binding Site." *Biochemistry* 59 (15): 1527–36.
- 514 Köhler, Simone, Michal Wojcik, Ke Xu, and Abby F. Dernburg. 2020. "Dynamic Molecular
515 Architecture of the Synaptonemal Complex." *BioRxiv*. bioRxiv.
516 <https://doi.org/10.1101/2020.02.16.947804>.
- 517 Kursel, Lisa E., Jesus E. Aguayo Martinez, and Ofer E. Rog. 2023. "A Suppressor Screen in *C.*
518 *Elegans* Identifies a Multi-Protein Interaction Interface That Stabilizes the Synaptonemal
519 Complex." *BioRxiv*. <https://doi.org/10.1101/2023.08.21.554166>.
- 520 Kursel, Lisa E., Henry D. Cope, and Ofer Rog. 2021. "Unconventional Conservation Reveals
521 Structure-Function Relationships in the Synaptonemal Complex." *ELife* 10 (November).
522 <https://doi.org/10.7554/eLife.72061>.

- 523 Kursel, Lisa E., Jesus E. Aguayo Martinez, and Ofer Rog. 2023. "A Suppressor Screen in *C.*
524 *Elegans* Identifies a Multiprotein Interaction That Stabilizes the Synaptonemal Complex."
525 *Proceedings of the National Academy of Sciences of the United States of America* 120
526 (50): e2314335120.
- 527 Labella, Sara, Alexander Woglar, Verena Jantsch, and Monique Zetka. 2011. "Polo Kinases
528 Establish Links between Meiotic Chromosomes and Cytoskeletal Forces Essential for
529 Homolog Pairing." *Developmental Cell* 21 (5): 948–58.
- 530 Little, Jordan, Maria Chikina, and Nathan L. Clark. 2024. "Evolutionary Rate Covariation Is a
531 Reliable Predictor of Co-Functional Interactions but Not Necessarily Physical
532 Interactions." *eLife* 12 (February). <https://doi.org/10.7554/eLife.93333>.
- 533 MacQueen, Amy J., Mónica P. Colaiácovo, Kent McDonald, and Anne M. Villeneuve. 2002.
534 "Synapsis-Dependent and -Independent Mechanisms Stabilize Homolog Pairing during
535 Meiotic Prophase in *C. Elegans*." *Genes & Development* 16 (18): 2428–42.
- 536 Mirdita, Milot, Konstantin Schütze, Yoshitaka Moriwaki, Lim Heo, Sergey Ovchinnikov, and
537 Martin Steinegger. 2022. "ColabFold: Making Protein Folding Accessible to All." *Nature*
538 *Methods* 19 (6): 679–82.
- 539 Nayak, Sudhir, Fernando E. Santiago, Hui Jin, Debbie Lin, Tim Schedl, and Edward T. Kipreos.
540 2002. "The *Caenorhabditis Elegans* Skp1-Related Gene Family: Diverse Functions in
541 Cell Proliferation, Morphogenesis, and Meiosis." *Current Biology: CB* 12 (4): 277–87.
- 542 Ouni, Ikram, Karin Flick, and Peter Kaiser. 2010. "A Transcriptional Activator Is Part of an SCF
543 Ubiquitin Ligase to Control Degradation of Its Cofactors." *Molecular Cell* 40 (6): 954–64.
- 544 Page, Scott L., and R. Scott Hawley. 2004. "The Genetics and Molecular Biology of the
545 Synaptonemal Complex." *Annual Review of Cell and Developmental Biology* 20: 525–
546 58.
- 547 Page, Scott L., Radhika S. Khetani, Cathleen M. Lake, Rachel J. Nielsen, Jennifer K. Jeffress,
548 William D. Warren, Sharon E. Bickel, and R. Scott Hawley. 2008. "Corona Is Required
549 for Higher-Order Assembly of Transverse Filaments into Full-Length Synaptonemal
550 Complex in *Drosophila* Oocytes." *PLoS Genetics* 4 (9): e1000194.
- 551 Phillips, Carolyn M., Kent L. McDonald, and Abby F. Dernburg. 2009. "Cytological Analysis of
552 Meiosis in *Caenorhabditis Elegans*." *Methods in Molecular Biology* 558: 171–95.

- 553 Rao, H. B. D. Prasada, Huanyu Qiao, Shubhang K. Bhatt, Logan R. J. Bailey, Hung D. Tran,
554 Sarah L. Bourne, Wendy Qiu, et al. 2017. “A SUMO-Ubiquitin Relay Recruits
555 Proteasomes to Chromosome Axes to Regulate Meiotic Recombination.” *Science* 355
556 (6323): 403–7.
- 557 Rillo-Bohn, Regina, Renzo Adilardi, Therese Mitros, Barış Avşaroğlu, Lewis Stevens, Simone
558 Köhler, Joshua Bayes, et al. 2021. “Analysis of Meiosis in *Pristionchus Pacificus* Reveals
559 Plasticity in Homolog Pairing and Synapsis in the Nematode Lineage.” *ELife* 10
560 (August): e70990.
- 561 Rog, Ofer, Simone Köhler, and Abby F. Dernburg. 2017. “The Synaptonemal Complex Has
562 Liquid Crystalline Properties and Spatially Regulates Meiotic Recombination Factors.”
563 *ELife* 6 (January). <https://doi.org/10.7554/eLife.21455>.
- 564 Sánchez-Sáez, Fernando, Laura Gómez-H, Orla M. Dunne, Cristina Gallego-Páramo, Natalia
565 Felipe-Medina, Manuel Sánchez-Martín, Elena Llano, Alberto M. Pendas, and Owen R.
566 Davies. 2020. “Meiotic Chromosome Synapsis Depends on Multivalent SYCE1-
567 SIX6OS1 Interactions That Are Disrupted in Cases of Human Infertility.” *Science*
568 *Advances* 6 (36). <https://doi.org/10.1126/sciadv.abb1660>.
- 569 Schild-Prüfert, Kristina, Takamune T. Saito, Sarit Smolikov, Yanjie Gu, Marina Hincapie, David E.
570 Hill, Marc Vidal, Kent McDonald, and Monica P. Colaiácovo. 2011. “Organization of the
571 Synaptonemal Complex during Meiosis in *Caenorhabditis Elegans*.” *Genetics* 189 (2):
572 411–21.
- 573 Schindelin, Johannes, Ignacio Arganda-Carreras, Erwin Frise, Verena Kaynig, Mark Longair,
574 Tobias Pietzsch, Stephan Preibisch, et al. 2012. “Fiji: An Open-Source Platform for
575 Biological-Image Analysis.” *Nature Methods* 9 (7): 676–82.
- 576 Schramm, Sabine, Johanna Fraune, Ronald Naumann, Abraham Hernandez-Hernandez,
577 Christer Höög, Howard J. Cooke, Manfred Alsheimer, and Ricardo Benavente. 2011. “A
578 Novel Mouse Synaptonemal Complex Protein Is Essential for Loading of Central
579 Element Proteins, Recombination, and Fertility.” *PLoS Genetics* 7 (5): e1002088.
- 580 Schrodinger, L. L. C. 2015. “The PyMOL Molecular Graphics System.” *Version* 1: 8.
- 581 Shin, Yongdae, and Clifford P. Brangwynne. 2017. “Liquid Phase Condensation in Cell
582 Physiology and Disease.” *Science* 357 (6357). <https://doi.org/10.1126/science.aaf4382>.

- 583 Smolikov, Sarit, Andreas Eizinger, Kristina Schild-Prufert, Allison Hurlburt, Kent McDonald,
584 Joanne Engebrecht, Anne M. Villeneuve, and Mónica P. Colaiácovo. 2007. "SYP-3
585 Restricts Synaptonemal Complex Assembly to Bridge Paired Chromosome Axes during
586 Meiosis in *Caenorhabditis Elegans*." *Genetics* 176 (4): 2015–25.
- 587 Smolikov, Sarit, Kristina Schild-Prüfert, and Mónica P. Colaiácovo. 2009. "A Yeast Two-Hybrid
588 Screen for SYP-3 Interactors Identifies SYP-4, a Component Required for Synaptonemal
589 Complex Assembly and Chiasma Formation in *Caenorhabditis Elegans* Meiosis." *PLoS*
590 *Genetics* 5 (10): e1000669.
- 591 Sternberg, Paul W., Kimberly Van Auken, Qinghua Wang, Adam Wright, Karen Yook, Magdalena
592 Zarowiecki, Valerio Arnaboldi, et al. 2024. "WormBase 2024: Status and Transitioning to
593 Alliance Infrastructure." *Genetics* 227 (1). <https://doi.org/10.1093/genetics/iyae050>.
- 594 Wang, Yixing, Hong Wu, Genqing Liang, and Ming Yang. 2004. "Defects in Nucleolar Migration
595 and Synapsis in Male Prophase I in the Ask1-1 Mutant of *Arabidopsis*." *Sexual Plant*
596 *Reproduction* 16 (6): 273–82.
- 597 Willems, Andrew R., Michael Schwab, and Mike Tyers. 2004. "A Hitchhiker's Guide to the Cullin
598 Ubiquitin Ligases: SCF and Its Kin." *Biochimica et Biophysica Acta* 1695 (1–3): 133–70.
- 599 Wong, Philip, Sonja Althammer, Andrea Hildebrand, Andreas Kirschner, Philipp Pagel, Bernd
600 Geissler, Pawel Smialowski, et al. 2008. "An Evolutionary and Structural
601 Characterization of Mammalian Protein Complex Organization." *BMC Genomics* 9
602 (December): 629.
- 603 Yang, Xiaohui, Ljudmilla Timofejeva, Hong Ma, and Christopher A. Makaroff. 2006. "The
604 *Arabidopsis* SKP1 Homolog ASK1 Controls Meiotic Chromosome Remodeling and
605 Release of Chromatin from the Nuclear Membrane and Nucleolus." *Journal of Cell*
606 *Science* 119 (Pt 18): 3754–63.
- 607 Zhang, Liangyu, Simone Köhler, Regina Rillo-Bohn, and Abby F. Dernburg. 2018. "A
608 Compartmentalized Signaling Network Mediates Crossover Control in Meiosis." *ELife* 7
609 (March). <https://doi.org/10.7554/eLife.30789>.
- 610 Zhang, Zhenguo, Songbo Xie, Ruoxi Wang, Shuqun Guo, Qiuchen Zhao, Hui Nie, Yuanyuan
611 Liu, et al. 2020. "Multivalent Weak Interactions between Assembly Units Drive
612 Synaptonemal Complex Formation." *The Journal of Cell Biology* 219 (5).
613 <https://doi.org/10.1083/jcb.201910086>.

- 614 Zheng, Ning, Brenda A. Schulman, Langzhou Song, Julie J. Miller, Philip D. Jeffrey, Ping Wang,
615 Claire Chu, et al. 2002. "Structure of the Cul1–Rbx1–Skp1–F BoxSkp2 SCF Ubiquitin
616 Ligase Complex." *Nature* 416 (6882): 703–9.
- 617 Zickler, Denise, and Nancy Kleckner. 2015. "Recombination, Pairing, and Synapsis of Homologs
618 during Meiosis." *Cold Spring Harbor Perspectives in Biology* 7 (6).
619 <https://doi.org/10.1101/cshperspect.a016626>.